RSC Advances

ROYAL SOCIETY OF CHEMISTRY

www.rsc.org/advances

Synthesis and Investigation of Water-soluble Anticoagulant Warfarin/Ferulic Acid grafted Rare Earth oxides Nanoparticles Materials

Mei-Ling Yang[1,2], Yu-Min Song[1*]

1 College of Chemistry and Chemical Engineering, Northwest Normal University, Lanzhou 730070

2 Department of Applied Chemistry, Yuncheng University, Yuncheng 044000

Graphic	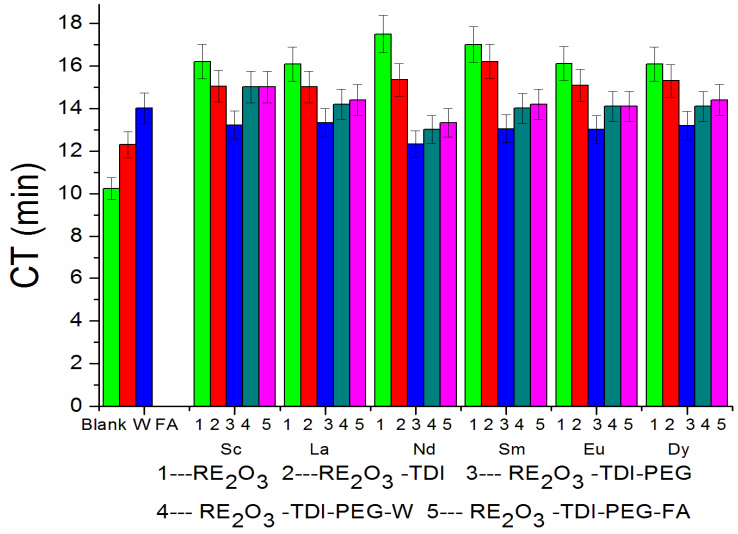
Text	**The synthesized warfarin/ferulic acid grafted rare rarth oxides nanoparticles materials have good solubility and better anticoagulant property.**

Synthesis and Investigation of Water-soluble Anticoagulant Warfarin/Ferulic Acid grafted Rare Earth oxides Nanoparticles Materials

Mei-Ling Yang[1,2], Yu-Min Song[1*]

1 College of Chemistry and Chemical Engineering, Northwest Normal University, Lanzhou 730070

2 Department of Applied Chemistry, Yuncheng University, Yuncheng 044000

[*] Corresponding author. E-mail: songym@nwnu.edu.cn (Prof. Y. M. Song)

Tel:+86-931-7972509;

Abstract:

To overcome the poor solubility of anticoagulant nano-rare earth (RE) oxides and warfarin/ferulic acid in water, two series of water-soluble anticoagulant materials RE_2O_3-TDI-PEG-warfarin and RE_2O_3-TDI-PEG-ferulic acid (TDI=Toluene 2,4-diisocyanate, RE=La, Eu, Nd, Sc, Sm, Dy) were prepared via the grafting method. The novel materials were characterized by IR, TG, XRD, SEM, TEM, ^{1}H and ^{13}C NRM and particle size test. The results confirmed that warfarin and ferulic acid were successfully modified onto the surface of rare earth nano-oxides. The anticoagulant properties were evaluated by coagulation time (CT), recalcification time (RT), activated partial thromboplastin time (APTT) and prothrombin time (PT). It was demonstrated that the novel hybrid materials have better cell compatibility and anticoagulant action than that of warfarin sodium or ferulic acid, due to the increased solubility (> 10 mg/mL) in water and synergism between nano-RE_2O_3 and warfarin/ferulic acid. It was also found that the anticoagulant time of the hybrid materials depends on the concentration as the higher the concentrations of hybrid materials, the longer the anticoagulant time. Addtionally, Sc_2O_3-TDI-PEG-warfarin and Sc_2O_3-TDI-PEG-ferulic acid exhibited the best anticoagulant properties, which indicates the potential application in the medicinal area. These results also provide the opportunity for the development of anticoagulant complexes and the potential application in other related fields.

Keyword: Water-soluble; Anticoagulant; Hybrid material; Warfarin; Ferulic acid; Rare earth nano-oxides

1. Introduction

Warfarin (W) and ferulic acid (FA) have long been the major drugs for anticoagulant in clinical applications [1-3]due to their advantages of oral availability, convenient application, inexpensive price, and lasting effect (Scheme 1). However, Shouming Wang [4]pointed out that there are a few drawbacks from the extended use of warfarin compounds as anticoagulant drugs, such as spontaneous bleeding and skeletal development retardation. Meanwhile, FA is widely studied in combination therapies in treating cancer, myocardial infarction, atherosclerosis [5]acute cerebral infarction [6]and for kidney protection [7]. However the application of FA in clinics is limited by its difficulty in penetrating the biological membrane bilayerd, and the poor solubility in water. Therefore, it is worth looking for a substitute that has lower toxicity, better anticoagulant properties and fewer side effects compared to warfarin/ferulic acid and their derivatives. One useful strategy to improve the efficiency of warfarin and ferulic acid is to fabricate hybrid materials by introducing new components. Studies on the properties of warfarin complexes composited with rare earth complexes[8] or transition metal[9] by Jiao and Dong groups has been demonstrated that these complexes exhibit better hemorrhagic anticoagulant properties, lower toxicity and high stability. Meanwhile, complexes of ferulic acid with transition metal or rare earth ions were found to prolong the anticoagulant time and recalcification time.[10] However, the poor water solubility still limits their applications in the clinical sense.

Rare earth complexes including rare earth nano-oxides as anticoagulants have been broadly investigated[11, 12]. For example, recently, Wang and co-workers [13] presented the anticoagulant performance of heparin/rare earth nano-oxide hybrids. Ni and Zhou [14, 15] et al. reported that the rare earth elements can replace Ca^{2+} to inhibit the coagulation of blood.

Though the rare earth nano-oxide, ferulic acid and warfarin have the significant anticoagulant effect, they suffer from poor water-solubility along with the problem of spontaneous bleeding due to large amounts of drug usage. As a result, it would be interesting to develop novel anticoagulant materials with high water solubility and a

small amount usage of drugs. Following this idea, herein two series of water-soluble RE_2O_3-TDI-PEG-Warfarin and RE_2O_3-TDI-PEG-Ferulic acid were prepared (Figure 1) by combining water-soluble H_2N-PEG-NH_2 to RE_2O_3 nano-particles and ferulic acid/warfarin. These novel hybrid materials were characterized by infrared spectra (IR), thermo-gravimetric analysis (TG), scanning electron microscope (SEM), powder X-ray diffractometry (powder-XRD), transmission electron microscope (TEM),1H and 13C NMR and particle size analysis. The anticoagulant properties were evaluated by anticoagulant time (CT), recalcification time (RT), activated partial thromboplastin time (APTT) and prothrombin time (PT). The results demonstrated that the novel hybrid materials have longer anticoagulation time than that of ferulic acid or warfarin, and the significantly improved water solubility (> 10 mg/mL) compared with bare ferulic acid (< 1 mg/mL) and warfarin (< 1 mg/mL). In addition, the cell adhesion of the materials remained the same as untreated control samples.

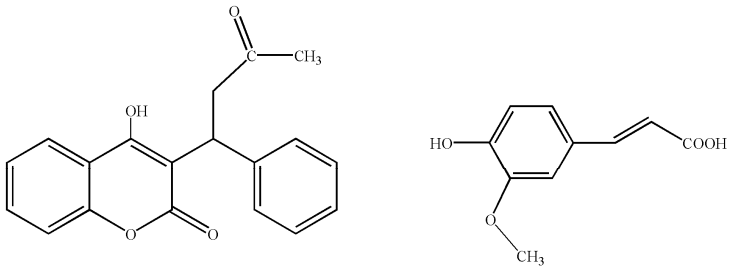

warfarin ferulic acid

Scheme. 1 The structure of warfarin and ferulic acid

2. Experimental

2.1 Materials and measurement

RE_2O_3 nano-oxides were purchased from Shanghai Yuelong Plant (China). Warfarin sodium was acquired from the Shanghai Sixteenth Pharmaceutical Factory (China) (m.p. 200~205□), and was treated with HCl to produce warfarin (m.p. 160.5~161.0□, literature[8]: 159.5~160.5□). Ferulic acid and PEG-4000 were obtained from Shanghai Zhongqin Chemical Reagent Limited Company (China). The H_2N-PEG-NH_2 was prepared according to the literature method.[16] Toluene 2, 4-diisocyanate (TDI) was acquired from Shanghai Kangda Amino acid Factory (China). All other chemicals and solvents were of analytical grade.

FT-IR spectra of the materials were obtained on Nicolet NEXUS 670 FT-IR spectrometer with the wave number range of 4000~400 cm^{-1} from KBr pellets. Thermogravimetric analysis (TG) was performed through a Perkin–Elmer TGA7 instrument in the flowing N_2 and the heated rate at 10□·min^{-1} in the 30-700□ range. The morphological features of all materials were identified through scanning electron microscopy (SEM) XL-20 (Philips, Netherlands). Transmission electron microscope (TEM) was used to determine the morphology of the hybrid materials. Powder X-ray diffraction (powder-XRD) analysis was obtained with a Philips XPert Pro diffract meter using Ni-filtered and Cu Kα radiation. Particle size analysis was performed on a Zetasizer Nano-Zs laser particle size instrument (Malvern, English). 1H and 13C NMR spectra were recorded using Bruker 400 MHz and d_6-DMSO as a solvent.

2.2 Modification of the surface of rare earth nano-oxides

The rare earth nano-oxides (RE_2O_3) were dried in a vacuum oven at 120□ for 7-8 h before use. RE_2O_3 (5 g), TDI (5 g) and 100 mL anhydrous acetone were added into a flask and sonicated under N_2 atmosphere for 2 h. To this solution, an appropriate amount of dibutyltin dilaurate was added and the solution was sonicated at 80 □ for 2 h. Finally, the reaction mixture was separated by filtration and the obtained solid was washed with anhydrous acetone (30 mL). The resulting materials were then roasted in a vacuum oven at 80□. The obtained solid was labeled as RE_2O_3-TDI, which is slightly soluble in water.

2.3 Preparation of warfarin/ ferulic acid rare earth nano-oxides hybrid materials

RE_2O_3-TDI (20 mg) was dissolved in chloroform (50 mL) and sonicated for 0.5 h. Then H_2N-PEG-NH_2 (100 mg) was added and the mixture was stirred at room temperature for 12 h before the addition of warfarin (10 mg) and anhydrous acetone (5 mL). The resulting mixture was refluxed for 12 h under N_2 at 70□. Upon completion of the reaction, the solid was separated by filtration, washed with diethyl ether (15 mL) and roasted in a vacuum oven at 45□ for 24 h. The obtained solid was marked as RE_2O_3-TDI-PEG-W, which is soluble in water (＞10 mg/mL) and some organic solvents, such as anhydrous ethanol, acetone, DMSO, etc.

According to similar manner, ferulic acid (13 mg), dimethylformamide (DMF, 15 mL), N, N'-dicyclohexylcarbodiimide (DCC, 13 mg) and N-hydroxyl succinimide (NHS, 11 mg) were added subsequently to the mixture of RE_2O_3-TDI and H_2N-PEG-NH_2 solution. The mixture was stirred for 12 h under N_2 at room temperature. Finally, the solid was separated by filtration and washed with diethyl ether (15mL) and roasted in a vacuum oven for 24 h at 45□. The obtained solid was marked as RE_2O_3-TDI-PEG-FA, which is soluble in water (＞10 mg/mL) and some organic solvents.

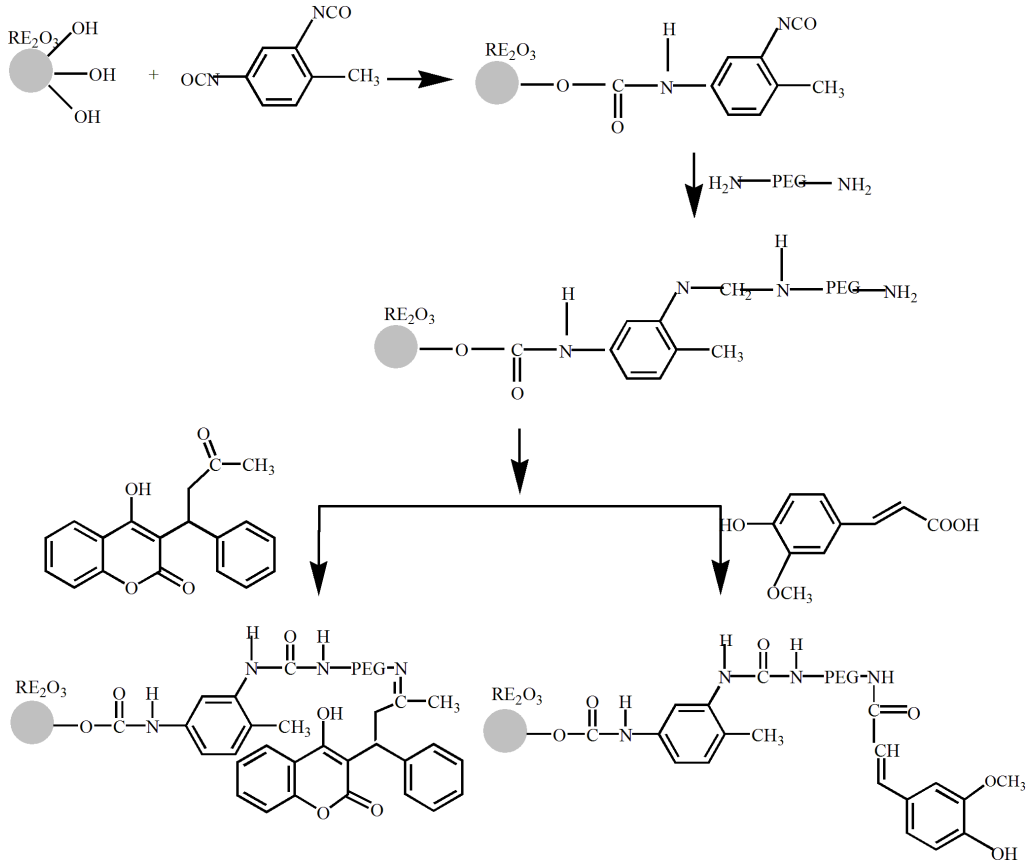

Fig.1 The preparation of the hybrid materials

2.4 Cell compatibility

The cell compatibility was measured by MTT (3-(4, 5-Dimethylthiazol-2-yl)-2, 5-diphenyltetrazolium bromide) method.[17] The HepG2 cells were routinely cultured in tissue culture boxes with 1640 culture medium (containing 10% fetal bovine serum), and incubated at 37□ in a humidified atmosphere with 95% air and 5% CO_2. After several generations of cells, the solution of hybrid materials (100 μL, 10mg/mL, by

diluting with 1640 culture medium) was added to the corresponding cell in the well, and then co-cultured at 37 °C for 48 h in a humidified atmosphere with 5% CO_2. After harvesting the cells, MTT solution (150 μL, 5 mg·mL^{-1}, PBS buffer solution) was added and the cell was cultured for 4h at 37 °C. After removing MTT solution, DMSO (150 μL) was added in each well at 37 °C, and the cell lysate was measured in a Bio-Rad Microplate Reader (model 1680) at excitation and emission wavelengths of 570 nm. The cell activity was expressed as a percentage of the optical absorbance of the test group vs the control group. [17]

2.5 Test of antclotting activity

2.5.1 Whole blood coagulation tests (CT)

Clotting time was determined visually at 37□ using eight groups of clean test tubes (three tubes in each group). The first group was blank and the other seven groups contained 10 mg of warfare sodium, ferulic acid, RE_2O_3, RE_2O_3-TDI, RE_2O_3-TDI-PEG, RE_2O_3-TDI-PEG-W, RE_2O_3-TDI-PEG-FA, respectively. All of the test tubes were maintained at a constant temperature of 37□. Healthy human blood (1 mL) was added to each tube. After 2 min, the test tubes were slightly warmed about 30° every 30 s until no more blood flow was observed at the constant temperature. The time between the addition of blood and no more blood flow was recorded as CT. To analyses the results about the test of antclotting activity, the SPSS(Statistical Product and Service Solution) softword version 16.0 is used. Standard deviation has been included for each sample and the value of significance of the differences(p) have been annotated in tables.

2.5.2 Recalcification time tests (RT)

The hybrid materials were dispersed in NaCl solution (0.154 mol·L^{-1}) for 24 h and then collected. Eight groups of clean test tubes (three tubes in each group) were used. The first group was blank and the rest of the seven groups contained samples (10 mg each). All samples were incubated at 37□ in a water bath for 2 min, then the pre-warmed mixture of blood plasma (1.0 mL) and $CaCl_2$ solution (0.3 mL, 0.025 mol·L^{-1}) were added into each test tube. A stainless steel crotchet was inserted in the solution and agitated tardily until the fibrin was formed (at 37□). The recalcification

time is defined as between the addition of the mixture and the formation of fibrin.

2.5.3 Anticoagulant activity test

The activated partial thromboplastin time (APTT) and prothrombin time (PT) indicate the influence of hybrid materials on the coagulant[18]. Blood plasma (0.5 mL) was added to the test tubes containing 10 mg of RE_2O_3-TDI-PEG-W or RE_2O_3-TDI-PEG-FA, respectively. The solution of $CaCl_2$ (0.25 mL, 0.025 $mol \cdot L^{-1}$) was then added to these tubes and incubated at 37 □ until the temperature was constant. The time of fibrin formation was recorded as APTT. The time of blood plasma clotting was recorded as PT, when PT agent was added to replace $CaCl_2$.

3. Results and discussion

3.1 Anticlotting properties

3.1.1 Whole blood coagulation tests (CT)

Fig.2 shows the CT of blank, nano-RE_2O_3, RE_2O_3-TDI, RE_2O_3-TDI-PEG, RE_2O_3-TDI-PEG-W and RE_2O_3-TDI-PEG-FA. Under the identical condition, the CT of the blank sample was the shortest one (about 10.24 min). The CT time of RE_2O_3-TDI-PEG-W (13.1-15.0 min) was longer than that of warfarin sodium (12.3 min), and the CT time of RE_2O_3-TDI-PEG-FA (14±0.5 min) was almost the same as that of ferulic acid (14.0 min). It was concluded that 6% (w %, $M_w/(M_{RE2O3}+ M_{TDI}+M_{PEG}+M_w)$,) warfarin or 4% ferulic acid in hybrid materials can achieve better or at least the same anticoagulant performance compared with the corresponding bare drug. Hence the hybrid materials are promising candidates for application in the medical field. It is interesting to note that the CT time of the samples was in the order of nano RE_2O_3>RE_2O_3-TDI>RE_2O_3-TDI-PEG-W/ RE_2O_3-TDI-PEG-FA>RE_2O_3-TDI-PEG. It may be because of greatly decrease the content of RE_2O_3 by introduced PEG.

The anticoagulant properties of RE_2O_3-TDI and RE_2O_3-TDI-PEG can be attributed to the nano RE_2O_3. RE_2O_3-TDI-PEG-W/ RE_2O_3-TDI-PEG-FA having longer CT time than that of RE_2O_3-TDI-PEG, due to the existence of warfarin/ ferulic acid. The CT time of Sc_2O_3-TDI-PEG-W and Sc_2O_3-TDI-PEG-FA was the longest in all of the

hybrid materials because of the similar chemical properties of Sc and Ca. The two elements are neighbors in the same period in the periodic table and the effective nuclear charge of Sc^{3+} is higher than the other rare earth ions. Therefore, Sc^{3+} can replace Ca^{2+} more easily than the other rare earth ions.

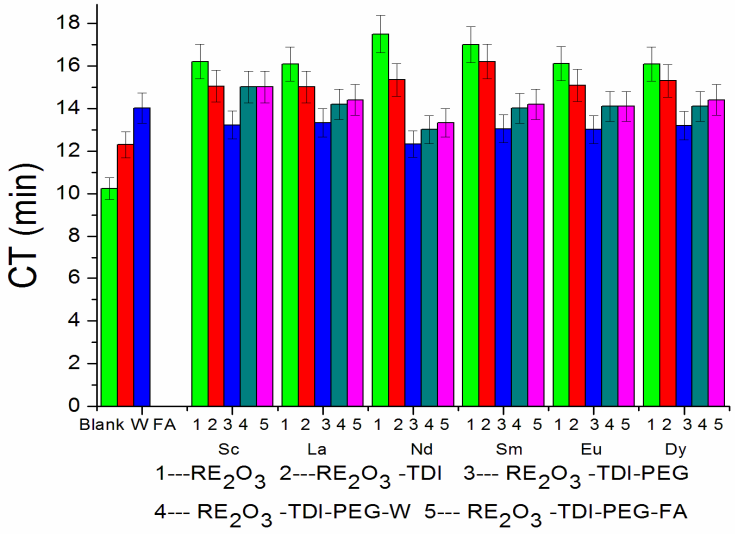

Fig.2 The coagulation time (CT) of different compounds

3.1.2 Test of recalcification time

Fig. 3 shows the recalcification time (RT) of warfarin sodium, ferulic acid and their hybrid materials. Under the identical condition, the RT of RE_2O_3-TDI-PEG-W (11.0-13.1 min) and RE_2O_3-TDI-PEG-FA (13.0-13.5 min) enhance significantly compared with the control sample (10 min), warfarin sodium and ferulic acid (11-12 min). The RT of RE_2O_3-TDI-PEG-W/RE_2O_3-TDI-PEG-FA is the longest in the group of nano-RE_2O_3 (11.2-12.0 min), RE_2O_3-TDI (10.2-12.0 min) and RE_2O_3-TDI-PEG (10.2-12.0 min). It is known that the longer the RT, the better the anticoagulant property. It can be therefore concluded here that the hybrid materials have better anticoagulant properties than that of RE_2O_3, warfarin sodium and ferluic acid. Additionally, Sc_2O_3-TDI-PEG-FA exhibited the best recalcification time, possibly due to its small radius and the highly effective nuclear charge of Sc^{3+}.

The CT and RT of the mixture of drugs and rare earth nano-oxides were also investigated. The results (Table 1) show the CT and RT of the mixture were shorter than those of the hybrid materials. Because there were about 50% (w %) drugs in the

mixture, it could not achieve the same anticoagulant performance compared with the hybrid materials (6% warfarin or 4% ferulic acid).

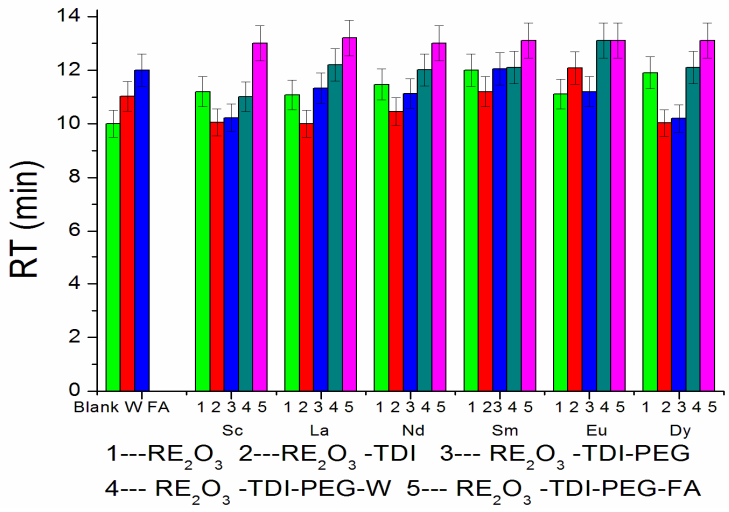

Fig.3 The recalcification time (RT) of various complexes

Table 1 CT (min) and RT (min) of the mixture of drug (5 mg, RE_2O_3,5 mgW/FA)

Mixture	CT /min	P	RT /min	P
Sc_2O_3+W	9.20(±0.02)	＜0.05	6.20(±0.02)	＜0.05
Sc_2O_3+FA	9.50(±0.02)	＜0.05	6.70(±0.02)	＜0.05
La_2O_3+W	9.00 (±0.02)	＜0.05	6.10 (±0.02)	＜0.05
La_2O_3+FA	9.50 (± 0.02)	＜0.05	6.50 (± 0.02)	＜0.05
Nd_2O_3+W	10.50(±0.02)	＜0.05	6.80(±0.02)	＜0.05
Nd_2O_3+FA	10.70(± 0.02)	＜0.05	7.30(± 0.02)	＜0.05
Sm_2O_3+W	9.80(±0.02)	＜0.05	7.00(±0.02)	＜0.05
Sm_2O_3+FA	10.10(±0.02)	＜0.05	7.50(±0.02)	＜0.05
Eu_2O_3+W	9.10 (±0.02)	＜0.05	6.10 (±0.02)	＜0.05
Eu_2O_3+FA	9.20(±0.02)	＜0.05	6.20(±0.02)	＜0.05
Dy_2O_3+W	9.30(±0.02)	＜0.05	7.10(±0.02)	＜0.05
Dy_2O_3+FA	9.20(±0.02)	＜0.05	7.30(±0.02)	＜0.05

3.1.3 Anticoagulant activity test

Table 2 the anticoagulant activity of hybrid materials (10 mg)

Compound	APTT /s	P	PT /s	P
Blank	27.50(±1)	＜0.05	12.40(± 1)	＜0.05
Sc_2O_3-TDI-PEG-W	34.20(± 2)	＜0.05	13.60(± 1)	＜0.05
Sc_2O_3-TDI-PEG-FA	33.70(± 2)	＜0.05	13.30(± 1)	＜0.05
La_2O_3-TDI-PEG-W	34.70(± 2)	＜0.05	13.50(± 1)	＜0.05
La_2O_3-TDI-PEG-FA	34.00(± 2)	＜0.05	13.20(± 1)	＜0.05
Nd_2O_3-TDI-PEG-W	36.50(± 2)	＜0.05	13.80(± 1)	＜0.05
Nd_2O_3-TDI-PEG-FA	33.20(± 2)	＜0.05	13.10(± 1)	＜0.05

Sm_2O_3-TDI-PEG-W	33.20(± 2)	＜0.05	13.20(± 1)	＜0.05
Sm_2O_3-TDI-PEG-FA	33.00(± 2)	＜0.05	13.20(± 1)	＜0.05
Eu_2O_3-TDI-PEG-W	34.70(± 2)	＜0.05	13.50(± 1)	＜0.05
Eu_2O_3-TDI-PEG-FA	34.20(± 2)	＜0.05	13.10(± 1)	＜0.05
Dy_2O_3-TDI-PEG-W	34.50(± 2)	＜0.05	13.60(± 1)	＜0.05
Dy_2O_3-TDI-PEG-FA	33.50(± 2)	＜0.05	13.10(± 1)	＜0.05
Reference	25-37		10-13	

APTT and PT are multi-purpose investigation of the coagulation activity in vivo and in vitro. The prolonging APTT and PT indicate that there is an unusual congenital clotting factor or a lacking of multiple clotting factors in the blood. The data in Table 2 shows: (1) APTT and PT of hybrid materials were longer than that of the blank sample, which means the hybrid materials had better anticoagulant properties; (2) The values of APTT and PT of the hybrid materials were within the normal scope (APTT: 25-27, PT: 10-13), which indicates there was no effect on the blood property when a small amount of hybrid materials were present. Thus these kinds of hybrid materials exhibit a potential application in the medical field.

3.1.4 Cell compatibility

Fig.4 indicates the HepG2 cell viability after seeded for 48 h in the solution of nano-Nd_2O_3, Nd_2O_3-TDI, Nd_2O_3-TDI-PEG, Nd_2O_3-TDI-PEG-W and Nd_2O_3-TDI-PEG -FA. It can be seen that all cells had similar activation compared with the blank sample. Additionally, it was found that the cell activity was the highest in the presence of nano-Nd_2O_3 and Nd_2O_3-TDI. It indicated the cell amplification was effectively promoted by nano-Nd_2O_3 and Nd_2O_3-TDI. After PEG was grafted onto the surface of Nd_2O_3-TDI, the cell activity is decreased. The data of cell activity showed that the cell toxicity was reduced and the cell compatibility was enhanced after warfarin and ferulic acid were grafted onto RE_2O_3-TDI-PEG. This illustrates these hybrid materials have low toxicity and higher cellular compatibility. The results of the HepG2 cell viability (Table 3) after 2 days of the other hybrid materials seeding show no more effects of the materials on the cell activity, which displays that the materials have as low toxicity as blank sample.

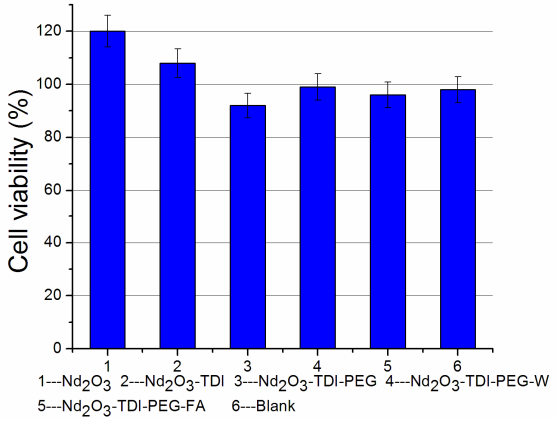

Fig.4 The HepG2 cell viability after 2 days of Nd hybrid materials seeding

Table 3 The HepG2 cell viability after 2 days of the hybrid materials seeding

Compound	Cell viability (%)	P
Sc_2O_3-TDI-PEG-W	94	＜0.05
Sc_2O_3-TDI-PEG-FA	92	＜0.05
La_2O_3-TDI-PEG-W	95	＜0.05
La_2O_3-TDI-PEG-FA	89	＜0.05
Nd_2O_3-TDI-PEG-W	99	＜0.05
Nd_2O_3-TDI-PEG-FA	96	＜0.05
Sm_2O_3-TDI-PEG-W	93	＜0.05
Sm_2O_3-TDI-PEG-FA	88	＜0.05
Eu_2O_3-TDI-PEG-W	90	＜0.05
Eu_2O_3-TDI-PEG-FA	94	＜0.05
Dy_2O_3-TDI-PEG-W	96	＜0.05
Dy_2O_3-TDI-PEG-FA	94	＜0.05
Blank	96	＜0.05

3.2 Characterization

3.2.1 FT-IR spectra

The novel hybrid materials were characterized by FT-IR. Due to similarity of the materials of RE_2O_3, here in nano-Eu_2O_3 was chosen as sample for detailed interpretation. The hydroxyl group in nano-Eu_2O_3 had the vibration absorption at 1620 cm^{-1} and 3400 cm^{-1}. The characteristic absorption of –NCO group of TDI appeared at 2270-2280 cm^{-1}. If the reaction occurs between the –NCO group of TDI and the hydroxyl in the surface of nano-Eu_2O_3, the absorption of –NH should appear at 3500-3300 cm^{-1}.

Fig. 5 (A) shows the IR spectra of Eu_2O_3-TDI. There was a vibration peak at

3300 cm^{-1}, which indicated the reaction has occurred. However, the presence of characteristic absorption of –NCO at 2273 cm^{-1} suggests that one of –NCO in the TDI was reserved. This group was used to react with H_2N-PEG-NH_2. [19] The IR spectra of Eu_2O_3-TDI revealed the presence of the carbonates absorption (1640 cm^{-1},1543 cm^{-1}), [20] the benzene absorption (1605 cm^{-1}), the ant-symmetric and symmetric stretching vibration peaks of the C-H of the TDI methyl (2922 cm^{-1} and 2857 cm^{-1}), all of which confirm the success of grafting TDI onto the surface of nano-Eu_2O_3.

Fig. 5 (B) shows the IR spectra of Eu_2O_3-TDI-PEG. The disappearance of the characteristic absorption of –NCO indicates that the –NCO left in the Eu_2O_3-TDI surface reacted with –NH of PEG. The characteristic vibration of PEG appeared at 2882 cm^{-1} ($v_{(C\text{-}C\text{-}H)}$) and 1109 cm^{-1} ($v_{(\text{-}C\text{-}O\text{-}C)}$), which confirmed the formation of Eu_2O_3-TDI-PEG.

Fig. 5 (C) reveals the IR spectra of warfarin. Two carbonyl absorption peaks appeared at 1718 cm^{-1} and 1664 cm^{-1}. [21] The former belongs to the ketone carbonyl stretching vibration; the latter is the vibration of the aromatic ring of carbonyl stretching, O–H stretching vibration appeared at 3283-3500 cm^{-1}.

In the IR spectra of Eu_2O_3-TDI-PEG-W (Fig. 5 (D)), the vibration of carbonyl stretching was absent, and –C=N absorption appeared at 1631 cm^{-1} , which suggested that the reaction between –C=O and $–NH_2$ has occurred and –C=N was formed consequently.

Fig. 5 (E) and Fig. 5 (F) illustrate the infrared spectra of ferulic acid and the hybrid materials Eu_2O_3-TDI-PEG-FA. The spectra showed that the vibration peak of carboxylic carbonyl appeared at 1686 cm^{-1} in the hybrid materials. This number shifted toward the lower wave number reaching to 1635 cm^{-1}, which indicated the formation of an amide bond between ferulic acid and $–NH_2$ of PEG. The results clearly suggest that ferulic acid has been grafted to the surface of nano-Eu_2O_3. The absorbance of the signal at 3425 cm^{-1} was stretching vibration of the phenol hydroxyl group. After forming the hybrid materials Eu_2O_3-TDI-PEG-FA, it became a smooth wide peak (3300 cm^{-1}-3600 cm^{-1}), which indicated the successful formation of ferulic acid hybrid materials. The results of the IR spectra of other samples were in

approximate agreement with that of Eu_2O_3-TDI-PEG-W and Eu_2O_3-TDI-PEG-FA (Table 4) .

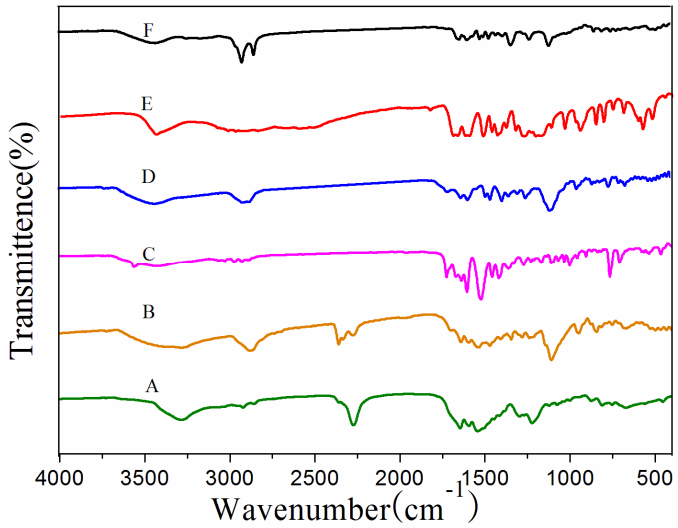

Fig.5 IR spectra of (A) Eu_2O_3-TDI (B) Eu_2O_3-TDI-PEG (C) Warfarin (D) Eu_2O_3-TDI-PEG-W (E) Ferulic Acid (F) Eu_2O_3-TDI-PEG-FA

Table 4 IR spectra(cm^{-1})

Compound	—C=O	—C=N
Warfarin	1718	---
Ferulic Acid	1686	---
Sc_2O_3-TDI-PEG-W	---	1627
Sc_2O_3-TDI-PEG-FA	1639	---
La_2O_3-TDI-PEG-W	---	1641
La_2O_3-TDI-PEG-FA	1651	---
Nd_2O_3-TDI-PEG-W	---	1647
Nd_2O_3-TDI-PEG-FA	1658	---
Sm_2O_3-TDI-PEG-W	---	1644
Sm_2O_3-TDI-PEG-FA	1656	---
Eu_2O_3-TDI-PEG-W	---	1631
Eu_2O_3-TDI-PEG-FA	1635	---
Dy_2O_3-TDI-PEG-W	---	1638
Dy_2O_3-TDI-PEG-FA	1646	---

3.2.2 Thermal analysis

Fig. 6 shows the weight loss curves of Eu_2O_3, Eu_2O_3-TDI, Eu_2O_3-TDI-PEG and Eu_2O_3-TDI-PEG-FA. The results show that the weight loss of TDI was about 31.9% (theory: 33.1%) in 200-300□. In 300-600□, the weight loss was mainly due to the decomposition and melting oxide of PEG and ferulic acid in the hybrid materials. The

thermo-gravimetric curves of Eu_2O_3-TDI-PEG-FA reveal two significant weight loss steps, which were most likely due to the burning of TDI and PEG-FA. This result supported the conclusion obtained from IR spectra that the surface of RE_2O_3 was coated by PEG and warfarin/ferulic acid molecules. The curve of the weight loss of Eu_2O_3-TDI-PEG-W and the other hybrid materials was very similar to Eu_2O_3-TDI-PEG-FA. The TGA-DTA data is listed in Table 5. There are a remarkable resemblance between Eu_2O_3-TDI-PEG-W, Eu_2O_3-TDI-PEG-FA and the other compounds during weightlessness.

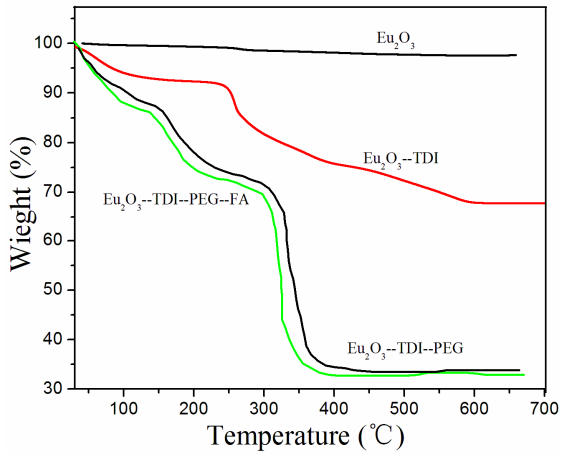

Fig.6 TGA curves

Table 5 the TG-DTA of the materials

Compounds	TDI-PEG-W losing temperature/℃, losing rate/% Found	TDI-PEG-FA losing temperature/℃, losing rate/% Found	Residual weight/% Found(calc.)
Eu_2O_3-TDI-PEG-W	300-600, 66.7		33.3
Eu_2O_3-TDI-PEG-FA		300-600, 65.4	34.6
Sc_2O_3-TDI-PEG-W	200-650, 77.5		12.5
Sc_2O_3-TDI-PEG-FA		200-650, 78.3	13.3
La_2O_3-TDI-PEG-W	4200-550, 70.0		29.6
La_2O_3-TDI-PEG-FA		200-550, 74.4	25.6
Nd_2O_3-TDI-PEG-W	200-550, 68.8		31.2
Nd_2O_3-TDI-PEG-FA		200-550, 67.4	32.6
Sm_2O_3-TDI-PEG-W	200-600, 67.6		32.4
Sm_2O_3-TDI-PEG-FA		200-600, 72.5	26.5
Dy_2O_3-TDI-PEG-W	200-550, 72.2		27.8
Dy_2O_3-TDI-PEG-FA		200-550, 71.2	26.8

3.2.3 ^{1}H NMR analysis

"^{1}H and ^{13}C NMR of the warfarin, ferulic acid, H_2N-PEG-NH_2, and La- materials

were investigated using d_6-DMSO as a solvent. Here the ^{1}H NMR chemical shifts of the main groups list as:

Ferulic acid: 3.83ppm. (—OCH_3), 6.37ppm (—CH=C—benzene), 7.54ppm (—benzene—CH=C), 9.57 ppm (—OH), 12.16 ppm. (—COOH); Warfarin : 2.12 ppm (—CH_3), 4.94 ppm (—CH_2), 11.39 ppm. (—OH); H_2N-PEG-NH_2: 2.49ppm (—NH_2), 3.33ppm (N—CH_2), 3.49ppm. (—CH_2); La-TDI-PEG-FA: 2.32 ppm. (—NH), 6.45ppm (—CH=C—benzene), 7.54ppm (—benzene—CH=C), 3.79ppm (—OCH_3), 10.51ppm (—OH); La-TDI -PEG-W: 2.32 ppm (—CH_3), 3.39 ppm (CH—N), 3.49 ppm (—CH_2), 10.45 ppm (—OH).

In La-TDI -PEG-FA, the peak at 12.38 disappeared, which was attributed to the –COOH group in the ferulic acid;[22] while the signals of —OCH_3 of ferulic acid and N—CH_2 of H_2N-PEG-NH_2 protons shifted slightly upfield; in La-TDI -PEG-W, the signals of —CH_3 of warfarin at 2.12ppm and N—CH_2 of H_2N-PEG-NH_2 at 3.33ppm were moved downfield. At the same time, the peak of –OH group of warfarin at 11.39ppm shifted upfeild to 10.45ppm. Hence suggesting the successful preparation of ferulic acid or warfarin was grafted onto nano-RE_2O_3 modified by H_2N-PEG-NH_2 and TDI.

The ^{13}C NMR chemical shifts of the main groups of ligands and La-complex list as: Ferulic acid: 116.74ppm (C=C—), 145.37ppm (—C=C), 170.01ppm(—COOH); Warfarin: 23.15ppm (—C(=O)—CH_3), 27.12ppm (—CH_3), 47.41ppm (—CH_2) ; H_2N-PEG-NH_2: 40.10 ppm (N—CH_2) , 70.20ppm (—CH_2); La_2O_3-TDI-PEG-W : 31.11 ppm (—CH_3), 36.20ppm (—C(=O)—CH_3), 40.17ppm (N—CH_2), 70.21ppm (—CH_2), 162.75ppm(N—C(=O)—N); La_2O_3-TDI-PEG-FA: 39.95 ppm (N—CH_2), 70.21ppm (—CH_2), 115.09ppm (C=C—), 138.18ppm (—C=C), 162.72ppm(N—C(=O)—N).

Obviously, when RE_2O_3-TDI-PEG-FA was formed, the peak of N—CH_2 at 40.10ppm of H_2N-PEG-NH_2, C=C— and —C=C of ferulic acid, at 116.74ppm and 145.37ppm, respectively, shifted weakly upfield; The peak of —COOH was attributed to ferulic acid at 170.01ppm which moved 162.72ppm because it was formed

acylamino group; in La-TDI -PEG-W, the signals of N—CH_2 at 40.10 ppm of H_2N-PEG-NH_2, —C(=O)—CH_3 and —CH_3 of Warfarin at 23.15ppm and 27.12ppm, respectively, shifted downfield. All of these phenomena show RE_2O_3-TDI-PEG-FA and RE_2O_3-TDI-PEG-W were successfully synthesized.

3.2.4 SEM analysis

The SEM images (Fig. 7) illustrate the morphology of the rare earth nano-oxides particles,PEG, La_2O_3-TDI-PEG-W and La_2O_3-TDI-PEG-FA. As shown in the SEM image, the nano-oxide particles had a spherical structure, which was significantly different from the plated PEG, flower structure of La_2O_3-TDI-PEG-W and La_2O_3-TDI-PEG-FA. It implies that the graft reaction has occurred on the surface of the rare earth nano-oxides and PEG-W /PEG-FA has completely enveloped the rare earth nano-oxides. However, in the La_2O_3 image of SEM, there are different size particles presence, which shows some aggregation existing in these particles.

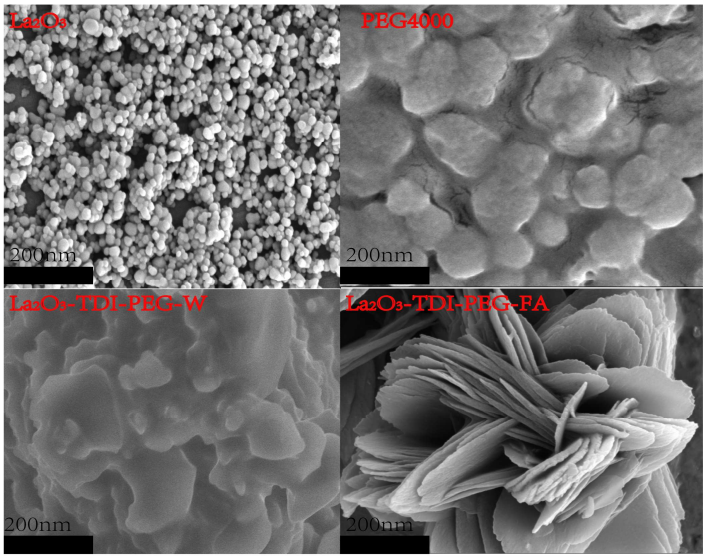

Fig.7 SEM images of compounds

3.2.5 TEM analysis

In the images (Fig.8) of TEM, the spherical black spots are metal particles and the white stripes are organic substances, the organic substance formed a skeleton and the

metal particles were evenly dispersed there. It can be seen the metal particles are packaged by organic molecules from the enlarged picture, which indicates that the title compound has been formed. In addition, it can be observed that there is different size particles existed in the TEM images, which due to the RE_2O_3 Nano- particles gathered and the organic substance parceled this particles loosely or tightly.

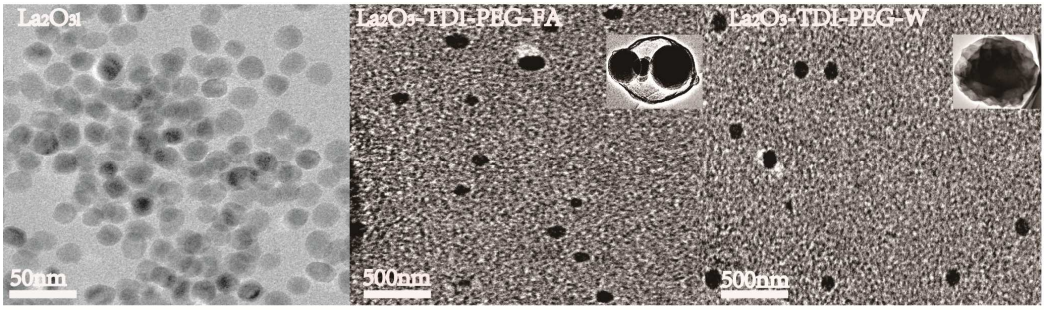

Fig.8 TEM images

3.2.6 XRD analysis

The powder X-ray diffractometry is a useful method for the detection of compounds in powder or microcrystalline states. Fig. 9 shows the X-ray diffraction patterns of warfarin sodium, ferulic acid, Dy_2O_3-TDI, Dy_2O_3-TDI-PEG-W and Dy_2O_3-TDI-PEG-FA. The XRD pattern of FA showed intense, sharp peaks at the diffraction angles (2θ) of 8.68° , 15.24° , 17.12° , 20.88° , and 26.16° , that proved the typical crystalline nature of the compound. Warfarin had strongest diffraction peaks at 7.84° ,15.64° ,21.2° , 25.44 and 29.92, implying its crystalline nature. On the other hand, the powder diffraction pattern of Dy_2O_3-TDI displayed several sharp peaks at 20.3° , 28.88° , 33.5° , 43.1° , 48.2° , 52.78° , and 57.2° , which indicates the compound exists as crystalline form. In the meantime, the powder diffraction pattern of Dy_2O_3-TDI-PEG-W and Dy_2O_3-TDI-PEG-FA were all lacking crystalline peaks, which means they are amorphous[23]. This may be due to the larger size of the hybrid material of Dy_2O_3-TDI-PEG-W and Dy_2O_3-TDI-PEG-FA, so they cannot easily form the regular structure.

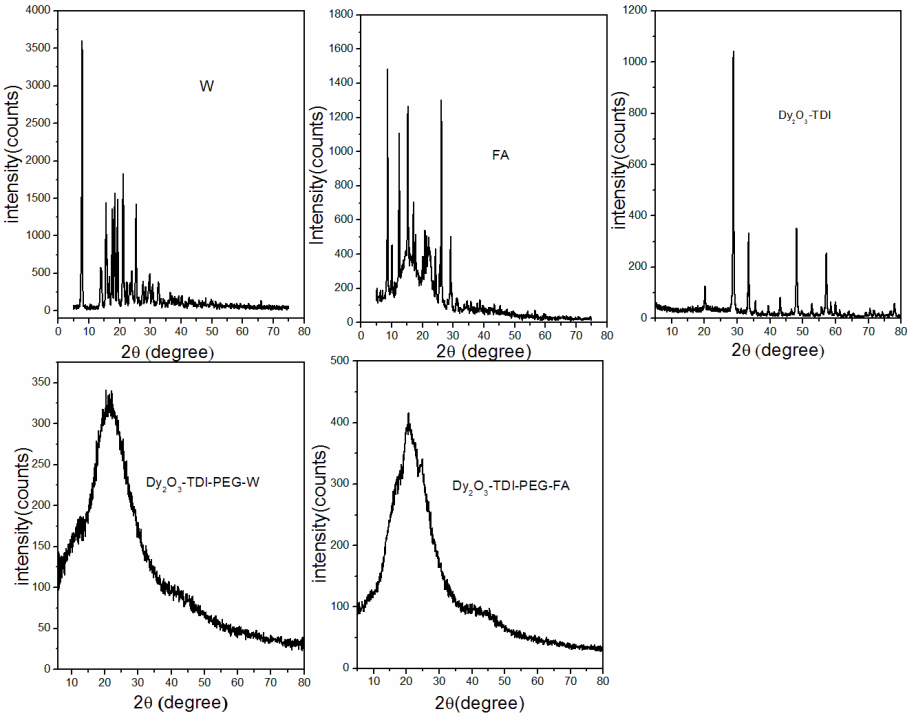

Fig.9 XRD of compouds

3.2.7 Particle size analysis

To confirm the successfully surface modification, the particle size of these hybrid materials was tested and analyzed by the Malvern's DTS software (version 6.0). When using this method to analysis samples, two values are given, a mean value for size (Z-Average), and a width parameter known as the Polydispersity Index (PDI). PDI is the particle size distribution coefficient and Z-Average (nm) is the average value of the particle diameter. The PDI and Z-Average values of Nd2O3-TDI and the hybrid materials are shown in Table 6.

Fig. 10 present the intensity (%) of the particle size for Nd_2O_3-TDI, Nd_2O_3-TDI-PEG, Nd_2O_3-TDI-PEG-W and Nd_2O_3-TDI-PEG-FA (0.01 mg·mL^{-1}, water) respectively. The value of Z-Average is 8.90 nm for Nd_2O_3-TDI), 200 nm for Nd_2O_3-TDI-PEG, 238 nm /214 nm for Nd_2O_3-TDI-PEG-W/ Nd_2O_3-TDI-PEG-FA. From Nd_2O_3, to hybrid materials, the Z-Average value becomes larger and larger, so warfarin (W) or ferulic acid (FA) has been grafted onto the nano-RE_2O_3 successfully by PEG.

Generally, it is believed when the value of PDI < 0.2, there is mainly a

monodisperse system. [24] However, the PDI values of all the samples are relatively over 0.2, which suggests that there is different size of particle existing in the test samples. This phenomenon is agreed with the results of SEM and TEM images.

Table 6 The PDI and Z- Average value of hybrid materials

Compounds	PDI	Z-Average (d.nm)	P
Eu_2O_3-TDI-PEG-W	0.533	181	<0.5
Eu_2O_3-TDI-PEG-FA	0.479	157	<0.5
Sc_2O_3-TDI-PEG-W	0.588	134	<0.5
Sc_2O_3-TDI-PEG-FA	0.578	120	<0.5
La_2O_3-TDI-PEG-W	0.680	174	<0.5
La_2O_3-TDI-PEG-FA	0.494	156	<0.5
Nd_2O_3-TDI-PEG-W	0.491	238	<0.5
Nd_2O_3-TDI-PEG-FA	0.446	214	<0.5
Sm_2O_3-TDI-PEG-W	0.468	224	<0.5
Sm_2O_3-TDI-PEG-FA	0.442	198	<0.5
Dy_2O_3-TDI-PEG-W	0.577	268	<0.5
Dy_2O_3-TDI-PEG-FA	0.469	247	<0.5
PEG-4000	0.494	116	<0.5

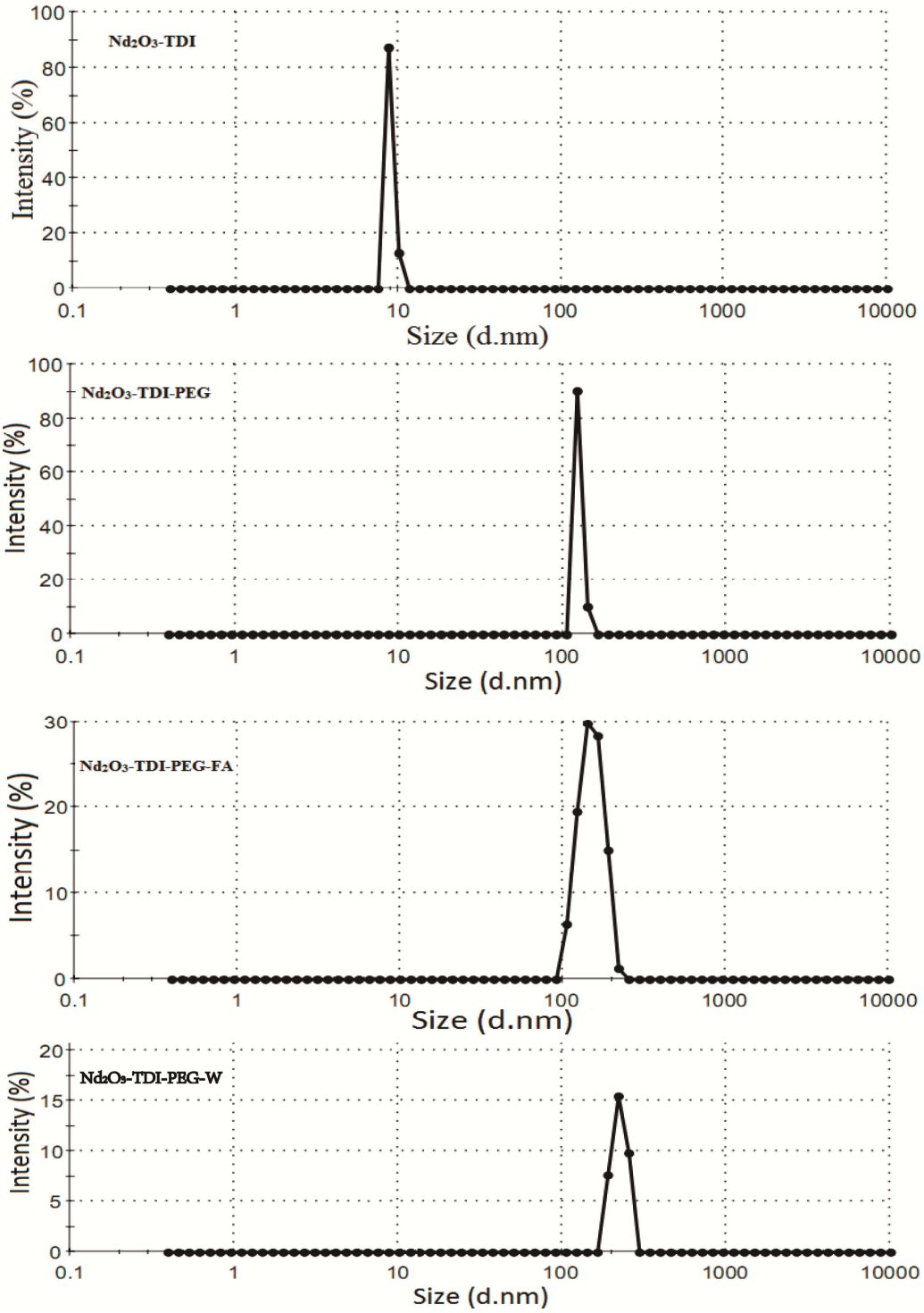

Fig.10 Particle size distribution of compounds

4. Conclusions

A class of water-soluble anticoagulant warfarin/ ferulic acid grafted rare earth nano-oxides hybrid materials was reported by using TDI and PEG as connection

reagents. The products were characterized by IR, TG, ^{1}H and ^{13}C NMR, XRD, SEM, TEM and particle size test. The results showed that warfarin / ferulic Acid were successfully grafted on the surface of the nano rare earth oxides. It was demonstrated that hybrid materials have better cell compatibility and anticoagulant property. The anticoagulant time, the recalcification time, the activated partial thromboplastin time and prothrombin time depend on the concentration. The higher the concentration of the hybrid material, the better the anticoagulant property. When a small amount of hybrid materials was added to the blood, no obvious variation of the properties of the blood was observed. These novel hybrid materials can serve as a foundation for clinical screening of anticoagulant drugs.

Reference：

[1] Eisaku Nomun, Ayumi Kashiwada, Asao Hosoda, *Bioorganic & Medicinal Chemistry,* 2003,**11**, 3807.

[2] Y. J. Hu, O. Y. Yu, C. M. Dai, *Biomacromolecules*, 2010,**11**, 106.

[3] T. B. Lu, M. Thomas, K. Shelley, *J. Med. Chem.* 2010, **53**, 1843.

[4] S. M. Wang, B. Richard, B. Tob, *J. Med. Chem.* 2010, **53**, 1465.

[6] Cecilia Anselmi, Marisanna Centini, Maurizio Ricci, etal., *J. Pharmaceut. Biomed.* 2006, **40,** 875.

[7] B.H. Wang,J.P. Ou-Yang, Cardiovasc, *Drug Rev.*,2005,**23**,161.

[8] T. Q. Jiao, J. G. Wu, F. L. Zeng, *Synth. React. Inorg.Metal-Organic Chim React.*, 1999, **29**, 725.

[9] Y. L. Dong, N. N. Luan, H. Y. Wang, Y. M. Song, *Acta Chemica Sinica*, 2008, **66**, 1497 in Chinese.

[10] P. Y. Wang, B. Wu., C. X. Bian, *Chin. J. Inorg. Chem.*, 2012, **28**, 1609 in Chinese.

[11] T. FUNAKOSHI, K. FURUSHIMA, H. SHIMADA, *Biochem. Inter.*, 1992, **28**, 113.

[12] L.J. Fu, J.X. Li, X.G. Yang, K.Wang, *J.Biol. Inorg. Chem.* 2009，**14**，219.

[13] K. J. Wang, H. X. Li, Y. M. Song, *Biopolymers*, 2010, **93**, 887.

[14] N. Xiang, X. M. Zhang, L. Y. Tian, *J. Biology*. 2009, **26**, 64.

[15] X. B. Zhou, Y. Z. Wei, *Chin. Bull. Life Sci.*, 1999, **11**, 70 in Chinese.

[16] B. D. Wang, C. J. Xu, J. *Am. Chem. Soc.*, 2008, **130**, 14437.

[17] X. F. Hu, J. Ji, *Acta Poly. Sin.,* 2009 ,**8**, 828.

[18] Sumit Kunar, Nesrin Alnasif, Emanuel Fleige, etal. *Eur. J. Pharm. Biopharm.*, 2014, **88**, 625.

[19] C. M. Wu, T. W. Xu, W.H. Yang, *J. Mem. Sci.*, 2003, **216**, 269.

[20] H. R. Li, J. Lin, H. J. Zhang, *Chem. Mater.*, 2002, **14**, 3651.

[21] E. J. Valente, E. C. Lingafeler, W. R. Porter, *J. Med. Chem.*, 1997, **20**, 1489.

[22] Bunzel, M., Ralph, J., Funk, C., & Steinhart, H., *Eur. Food Res. and Technol.*, 2003,**217**,128.

[23]G. Zingone, F. Rubessa. *Int. J.Pharm.*, 2005,**291**,5.

[24] Bohidar H.B., Behboudnia M. *Colloids Surf. A,* 2001,**178**, 313.